American Journal of Environmental Protection, 2020, Vol. 8, No. 1, 1-9
Available online at http://pubs.sciepub.com/env/8/1/1
Published by Science and Education Publishing
DOI:10.12691/env-8-1-1

Synoptic Analysis of Extreme Rainfall Event in West Africa: the Case of Linguère

Mouhammed Fall[1,*], Abdou Lahat Dieng[1], Saïdou Moustapha Sall[1], Youssouph Sane[2], Moussa Diakhaté[1]

[1]Laboratoire de Physique de l'Atmosphère et de l'Océan-Siméon Fongang (LPAO-SF),
École Supérieure Polytechnique, UniversitéCheikhAnta Diop,Dakar,Senegal
[2]Agence Nationale de l'Aviation Civile et de la Météorologie (ANACIM), Dakar,Senegal
*Corresponding author: mouhammed.fall@ucad.edu.sn

Received December 13, 2019; Revised January 28, 2020; Accepted February 15, 2020

Abstract After the drought period of the 70s and 80s, the Sahelian countries have experienced a resurgence of heavy rains phenomena and devastating floods causing a lot of socio-economic damages since the beginning of the 21st century. In this work, the environmental conditions associated with an extreme rainfall event that has led to high socio-economic impact in Senegal is studied by using the database of the extreme event from the DPC (Direction de la Protection Civil) of Senegal, Satellite products, ERA-Interim reanalysis and five Weather Model Prediction datasets. The rain event occurred on 26 August 2017 at Linguère (15.07°W and 15.23°N). This study aims to analyse the synoptic conditions associated to the event and also the ability of the numerical forecast models to predict it. The satellite dataset shows that the precipitating convective system was initiated at the level of a trough, on August 25 in the afternoon, and the extreme rain event took place on August 26 between 0600UTC and 1200UTC over Linguère. Various atmospheric parameters such as the configuration of the low-level moisture transport, precipitable water, relative humidity at 200 and 700-hPa as well as relative vorticity at 700-hPa appear as good indicators to characterize extreme rainfalls. The numerical forecast models used were able to predict short-term rainfall around Linguère. However, none of the models could predict the extreme aspect of precipitation because they tend to underestimate the intensity compared to rain gauge records.

Keywords: *extreme rainfall in the Sahel/Senegal, Meso-scale convective systems, moisture transport, precipitable water, relative humidity, wind, numerical forecast models*

Cite This Article: Mouhammed Fall, Abdou Lahat Dieng, Saïdou Moustapha Sall, Youssouph Sane, and Moussa Diakhaté, "Synoptic Analysis of Extreme Rainfall Event in West Africa: the Case of Linguère." *American Journal of Environmental Protection*, vol. 8, no. 1 (2020): 1-9. doi: 10.12691/env-8-1-1.

1. Introduction

After the severe drought period of the 1970s and 1980s, over the Sahelian countries there has been a return to normal conditions in the precipitation regime since the beginning of the 21st century [1,2,3,4]. However, the latter is associated with high variability of sub seasonal rainfall distribution (extreme rainfall, dry spells, high variability in the length of wet seasons, etc.) which is particularly pronounced in the western Sahel [5,6,7]. Based on observations, [8] shows evidence that in the Sahel, extreme rainfall events have become more numerous than during the 1950s and this feature is positively correlated with the signal of climate change. Reference [9] showed a significant increase in daily precipitation above the 95th percentile. In the Sahel, urban areas are particularly vulnerable to flooding. Reference [10] showed insufficient urban planning, which exposed a large part of the poor population living in these areas vulnerable to flooding. These phenomena of heavy rains and devastating floods cause inestimable socio-economic damages and losses. All these parameters contribute to the regression of the availability of human resources, to the inaccessibility of necessities leading to the speculation of foodstuffs [11].

To try reducing all these negative impacts linked to the phenomena of extreme rains, it would be essential to better document the environmental processes associated with extreme rains as well as their predictability in numerical forecast models. Some recent studies have been made to characterize this type of event; however, they only concerned about the case of Ouagadougou (September 2009) and of Dakar (August 2012) [12,13,14]. The case of Linguère is not documented to our knowledge even though it is reported to have led to manysocio-economic damages.

The Linguère event was a torrential rain of 218.6 mm, which fell on August 26, 2017, over Linguère, a city located in the north center of Senegal which is an area where floods are not frequent. Despite the fact that the event did not cause any loss of human life, it had a meaningful impact on socio-economical aspect. Several buildings were damaged and many domestic animals were taken away. In the streets, the decor is sinister: floating mattresses, also cabinets and appliances exposed to the sun.

Our objective is to study the specificity of an extreme rain event with high socio-economic impact, listed in the database of the Direction de la Protection Civil (DPC) of Senegal. The study is based on various datasets of observations and the diagnose of the ability of numerical forecast models to predict this event. This analysis will allow us, on the one hand, to characterize the dynamics of this event by trying to extract the main indicators and, on the other hand, to evaluate the predictability of some numerical forecasting models.

The paper is structured as follows. Firstly, we present the data used and the study area in Section 2; then we explain the methodology in Section 3 and finally the results are presented using two main points in Section 4. The first point is the analysis of the atmospheric dynamics using satellite observations and reanalysis data while the second refers to the predictability of the event in some numerical forecast models. Conclusions and perspectives are presented in Section 5.

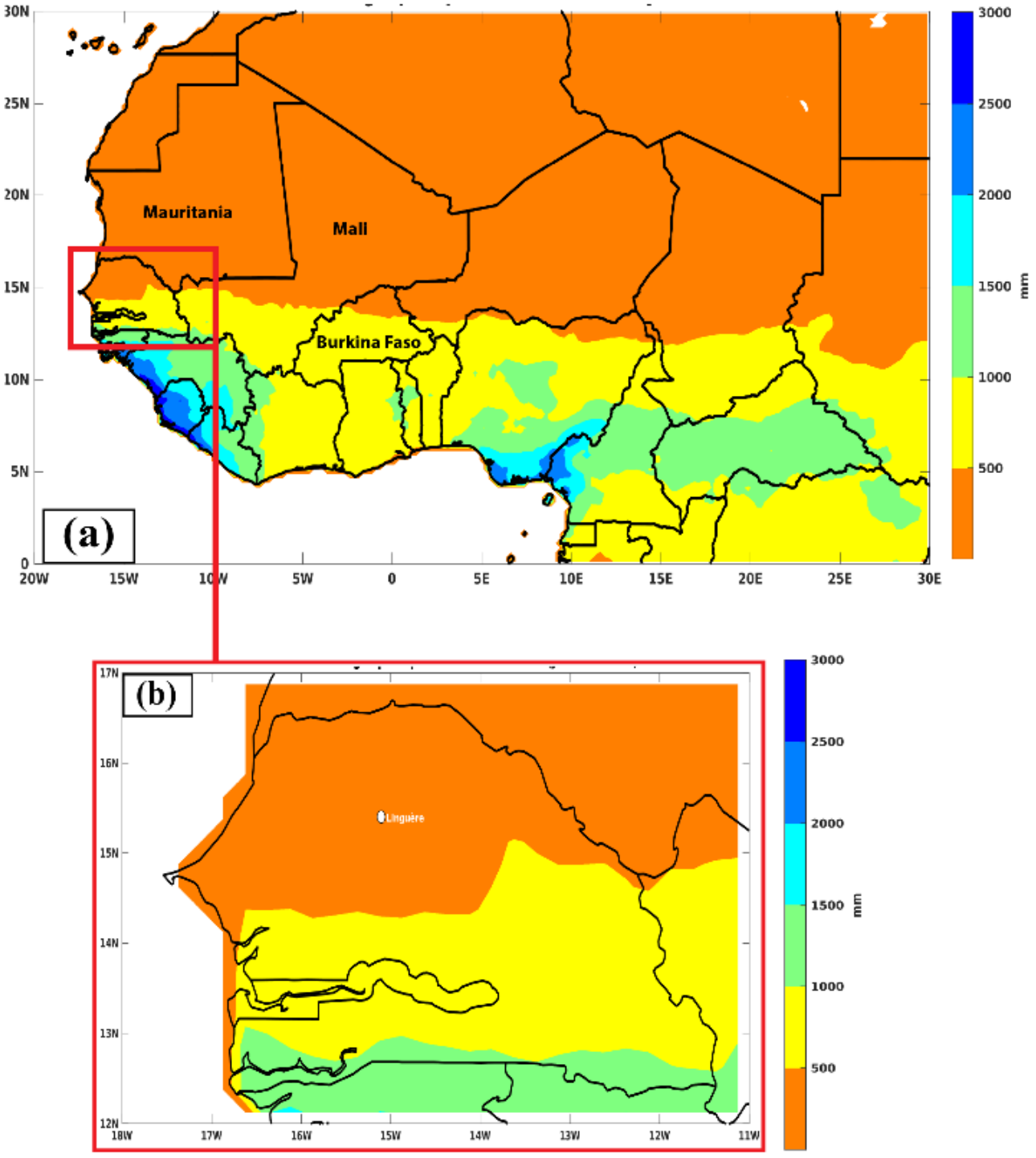

Figure 1. Climatology of precipitation for the period 1981-2010 between June and October by CHIRPS. **(a)** represents the West Africa zone and **(b)** the Senegal zone. The geographical position of Linguère is also show.

2. Data and Study Area

2.1. Study Zone

Senegal is located in the Western part of the Sahel between 12.5°-16.5° N and 12°-17° W (Figure 1(a)). It is characterized by two main seasons: a dry season (from November to April-May) marked by the predominance of maritime trade winds (in the west) and continental trade winds (in the interior); and a rainy season (from May - June to October), dominated by the flow of the West African monsoon [15,16,17]. The maximum rainfall is noted in August and September, coinciding with the period during which the intertropical convergence zone (ITCZ) reaches its northernmost position above Senegal [18]. The major element of the climate is the great spatial variability of precipitation, which fluctuates on average between more than 1000 mm in the South and less than 300 mm in the North over a year [19]. This gradient manifest itself mainly on the number of rainy days, which vary on average around 20 days in the north and 80 days in the south. The region of Linguère (15.07°W and 15.23°N), where the extreme rain event occurred, is located in the northern part of Senegal (Figure 1(b)).

2.2. Data

The DPC is attached to the Ministry of Interior of Senegal and is responsible for the prevention of risks of all kinds, as well as the protection of people, property and the environment against all claims and disasters. The DPC reports made it possible to identify the extreme meteorological case studied in this study.

The daily data used as reference to theamount of precipitation came from the AgenceNationale de l'Aviation Civile et de la Météorologie (ANACIM) of Senegal. The Linguère synoptic station was used to assess the amount of rain associated with the event.

Daily TRMM (Tropical Rainfall Measuring Mission) data from an equatorial orbit satellite for the observation of precipitation in the tropical band between 30°N and 30°S were used. The TRMM has strong repeatability over West Africa with around 8 passages per day. The data collected by TRMM are of great importance for understanding the tropical climate and its evolution. The project was launched on November 27, 1997, with the visible and infrared scanner (VIRS; 5 channels), the TRMM Microwave Imager (TMI; 9 channels) and the precipitation radar (PR) [20]. Reference [21] evaluated TRMM products in West Africa during the monsoon season and showed excellent agreement with station data. The performance of TRMM 3B42 V6 compared to others SRFEs in East and West Africa on a daily scale and at a 0.25° spatial scale,has been highlighted by [22]. Knowing that [23] and [24] provided the proof that V6 and V7 are rather comparable, therefore version 7 of the dataset 3B42 was used in this study for the spatial monitoring of precipitation. It provides an estimation of precipitation over 3 hours on a 0.25° grid.

The infrared (IR) Brightness Temperature (BT) data merged over 4 km are produced by the Climate Prediction Center (CPC) of the national environmental forecast center of NOAA. Each cooperating geostationary (geo) satellite operator, followed by the multifunctional transport satellite [MTSat], then Himawari, in Japan, and the meteorological satellite [Meteosat] (European community) transmits IR images to the CPC. Then, the global geo-IR are corrected according to the zenith angle [25], redirected for parallax and merged on a global grid. When duplicating data in a grid, the value with the smallest zenith angle is taken. The data are provided on a latitude/longitude grid equivalent to 4 km on the latitude band 60°N-S, and its temporal resolution is 30 minutes. The dataset was first produced in late 1999, but the current uniformly processed record was available on February 17, 2000.

The Climate Hazards InfraRed Precipitation with Station (CHIRPS) is a semi-global rainfall product designed for monitoring droughts and global environmental changes [26]. CHIRPS data cover most of the globe (50°S-50°N, all longitudes). The data period extends from 1981 to the present. The CHIRPS methodology uses satellite images at a resolution of 0.05° with data from meteorological stations to create a rainfall time series in a grid offering capabilities for analyzing trends and monitoring seasons. In this study daily CHIRPS rainfall data were used with a spatial resolution of 0.25º.

ERA-Interim (ERAI) integrates a large number of observations of all types, which allows a better description of the state of the atmosphere [27]. The reanalyses used in this work are available on a horizontal grid of 0.75° and 27 pressure levels. Reference [28] showed good agreement between these data and in-situ observations in Africa both on daily and synoptic scales.

Forecasting is very important to avoid huge damage from extreme rain events. For this, we studied the predictability of the case study, using the outputs of five different operational models with 0.5° x 0.5° spatial resolution.

The model of the ECMWF (European Center for Medium-Range Weather Forecasts) has the IFS (Integrated Forecast System), which provides the analysed and forecasted state of the atmosphere every day at noon (0000 and 1200 UTC).

The Korea Meteorological Administration (KMA) is the meteorological service of South Korea and likewise the ECMWF, its analyses are available at a time step of 12 hours (0000 and 1200 UTC).

The United Kingdom Met Office (UKMO) is the British national meteorological service, and its forecast model contains four 6-hourly time steps (0000, 0600, 1200, and 1800 UTC).

The National Centers for Environmental Prediction (NCEP) is a group of specialized national weather forecast centers in the United States. Their model also presents four 6-hourly time steps (0000, 0600, 1200, and 1800 UTC).

The Météo-France is the official meteorology and climatology service in France. Their forecasting model also has datasets available at 12-hour time steps but at 0600 and 1800 UTC.

3.Methods of Analysis

This study is interested in an extreme case of rain provided by the DPC reports, whichinclude the date, the

place and the impacts associated with this heavy rain. The study began with the analysis of satellite BT and TRMM precipitation data. This preliminary work allows us to follow the formation and progression of the cloud systems associated with the event and to detect the exact moment on the day when the heavy rains fall. A range of BT thresholds between 260K and 170K was taken as inspired by the studies of [29]. Thus, this temperature interval allows to characterize the convective system associated with the event.

Then the ERA-Interim atmospheric reanalyses were used to study the behavior of some meteorological parameters such as humidity transport as well as its divergence. In addition, precipitable water, relative humidity or wind datasets were used to see if they are good indicators for the characterization of the event.

The humidity transport T ($kg.m^{-2}.s^{-1}$) is calculated by considering the low layer of the atmosphere. We have integrated the product of specific humidity q ($kg.kg^{-1}$) and the wind V ($m.s^{-1}$) between the surface and 850-hPa.

$$T = \int_{Surf}^{850hPa} q.V \tag{1}$$

The precipitable water (PW) is the amount of water that could be obtained if all of the water vapor in an air column was condensed and precipitated. It is given in the form of the thickness or areal mass of liquid water ($kg.m^{-2}$).

$$PW = \frac{1}{g}\int_{Psfc}^{Ptop} qdp \tag{2}$$

With g = 9.81 $m.s^{-2}$ being the gravitational acceleration and Psfc (hPa) being the atmospheric pressure at the surface and Ptop represents the pressure at the top of the reanalysis atmospheric layer.

The relative humidity (Hr) is the ratio between the water vapor pressure present in the air (Pvap) and the saturating pressure value (Psat) and it is most often expressed as a percentage.

$$Hr = \frac{Pvap}{Psat} * 100 \tag{3}$$

The last step is, finally, to examine the predictability of the event through operational numerical forecast models. The periods for initializing the models are 3, 2 and 1 days before D-Day (DD),on August 26, 2017, and are considered to be short-term forecasts.

4. Results and Discussion

4.1. Comparison of Precipitation Data

Figure 2 represents the time series of the daily precipitation during August 2017 at Linguère, using in-situ data (red line) and TRMM (blue line) datasets and also the climatology of TRMM precipitation calculated over the period 2003-2017 during August (green curve). The analysis of these time series shows that in general the amount of daily rain rarely exceeds 20 mm while on August 26, 2017 (the D-Day) the rainfall estimated by TRMM was at about 130 mm (5 times greater than the normal). TRMM, therefore, captured the extreme, but compared to ground observations, it significantly underestimated the intensity of the event. The recorded rainfall during this day within ground station appears twice that from the satellite estimation (218.6mm). This distribution of precipitation shows the extreme nature of the rain of August 26, 2017, causing enormous damage noted in Linguère. The following sub-section documents the monitoring of the hourly evolution of dynamic and thermodynamic conditions associated with the extreme rain event.

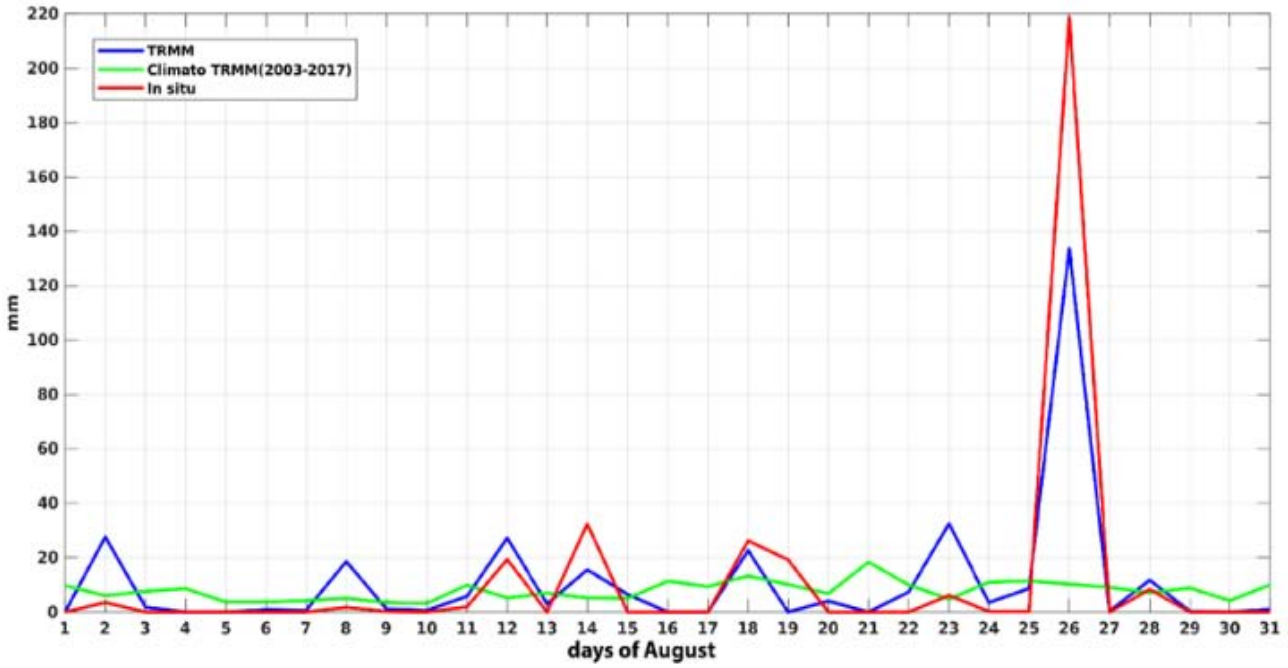

Figure 2. Climatology of TRMM precipitation of August for the period 2003-2017 (green) and daily precipitation of August 2017 with ground station data (red) and TRMM (blue).

4.2. Analysis of the Dynamics

Figure 3 shows the evolution of the TRMM hourly precipitation rate (in contours), IR BT (in color) and 850-hPa wind from August 25 at 1200 UTC to August 26 at 1800UTC. On August 25, 2017, at 1200 UTC (Figure 3(a)), the presence of a cyclonic circulation whose centre is located between Mali and Burkina Faso is noticed and a convection initiation took place in the afternoon between 1200 UTC and 1800 UTC (Figure 3(b)) in South Mauritania, near the borders between Mali and Senegal. The low value of BT (below 213K), shows an increase of convection during that period. This convective system is developing near an African Easterly Wave (AEW) trough with a strong low-level vortex. This configuration is consistent with the results from several observational studies suggesting that deep convection tends to occur in the vicinity of the AEW trough [30,31,32,33]. The precipitating system arrives at Linguère on August 26, 2017, around 0600 UTC and the extreme rain event mainly took place between 0600 UTC (Figure 3(d)) and 1200 UTC (Figure 3(e)). Between 1200 UTC and 1800 UTC of the same day (Figure 3(f)), the convective system continues to progress towards the west and begins to dissipate over the Atlantic Ocean (Figure 3 (e) and (f)).

After analyzing the evolution of the precipitating convective system associated with the wave and then detecting the time (between 0600 UTC and 1200 UTC), which the precipitating event occured, the behavior of a few atmospheric parameters associated with this extreme rain at Linguère has been analysed in order to better characterize the extreme event. Figure 4a represents the 850-hPa surface integrated humidity transport (current line), its divergence (isolines; solid contours represent positive values while the dashes show negative values) and the precipitable water (overlapped in color). During the event, around 0600 UTC, the presence of a cyclonic circulation of humidity transport centered in South Mauritania, lead to a strong convergence of humidity in that zone as well as in the western part of the vortex. Around 1200 UTC the center of the vortex is located southwest to its initial position. The humidity transport occurs from North to West of the geographical position of Linguère and the very northward position of the vortex perhaps explains the fact that in August the ITCZ is located above Senegal.

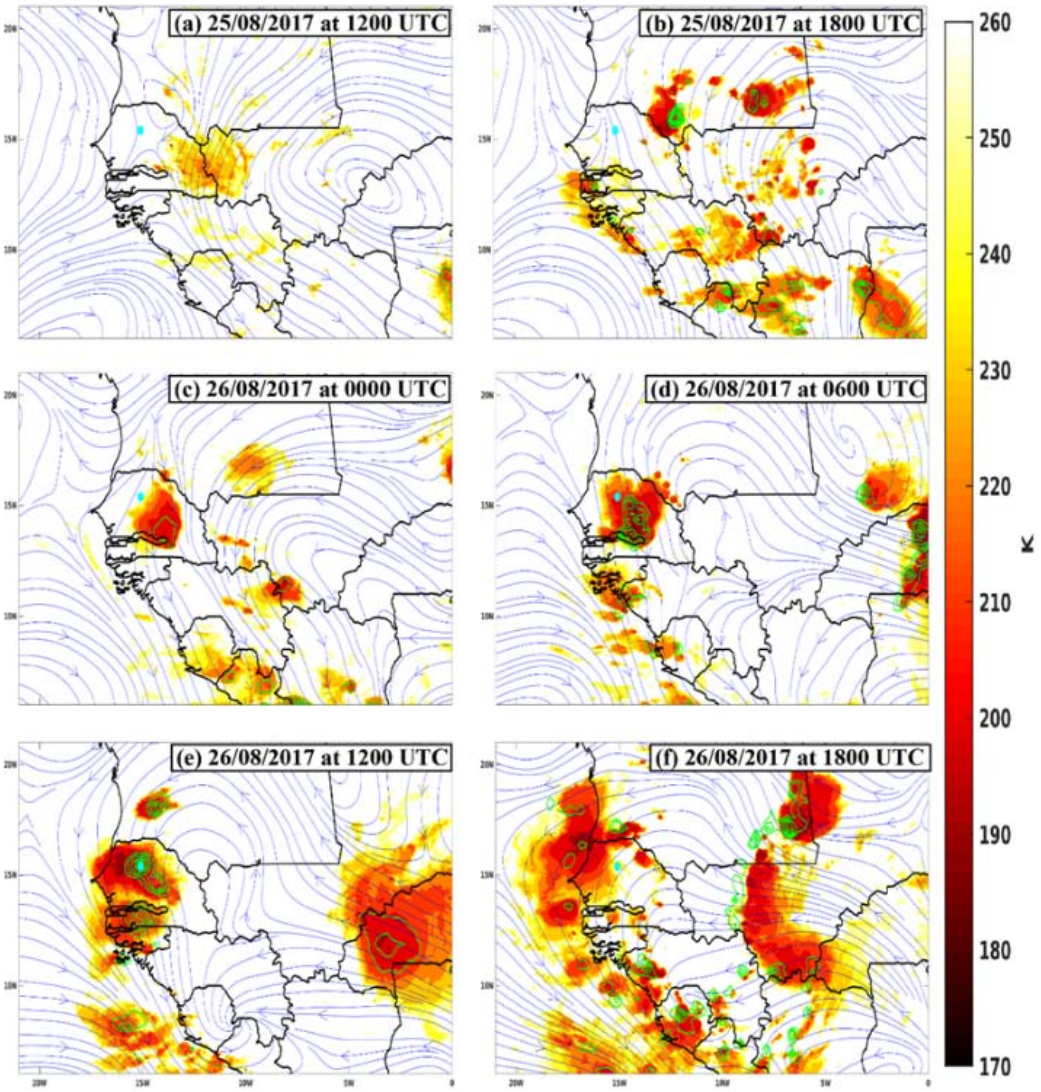

Figure 3. Monitoring of the evolution of the convective system using BT (in color), TRMM precipitation rate (in contour) and the 850-hPa ERAI wind (in streamlines) associated with the extreme rain event. The cyan point indicates the geographic position of Linguère.

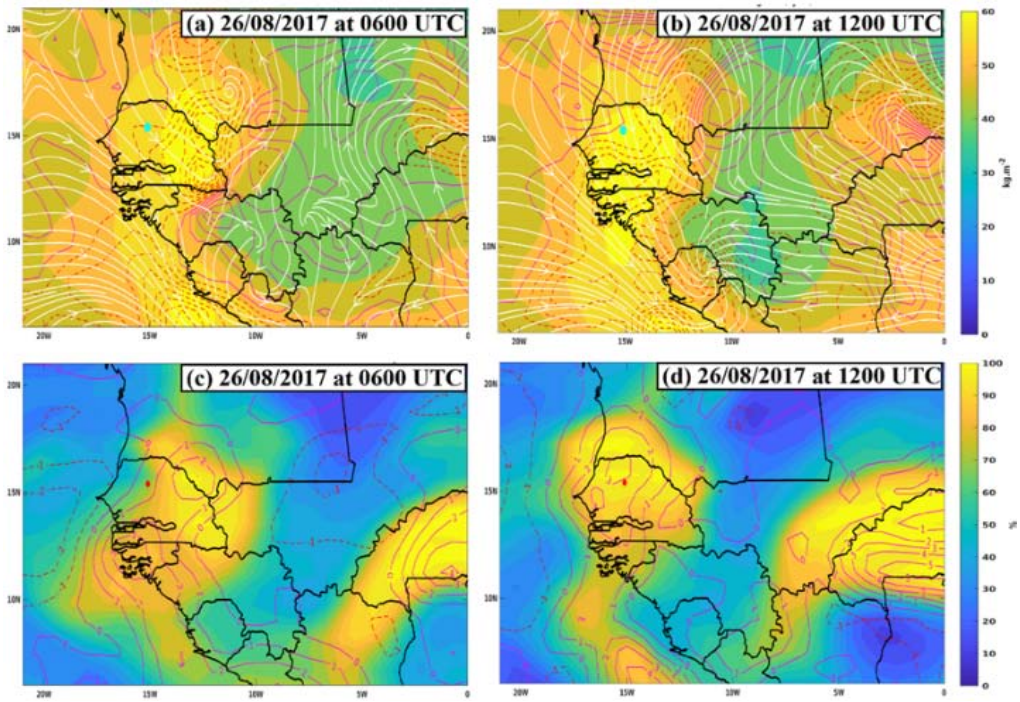

Figure 4. Composite of the 850-hPa surface integrated moisture transport (in streamline), divergence of 850-hPa surface integrated moisture transport (in outline) and precipitable water (in color) for 26/08/2017 at 0600UTC **(a)** and 1200UTC **(b)**. The wind divergence (in contour) and relative humidity at 200-hPa (in color) for 26/08/2017 at 0600UTC **(c)** and 1200UTC **(d)** are also represented. The cyan and red dots represent the geographical position of Linguère.

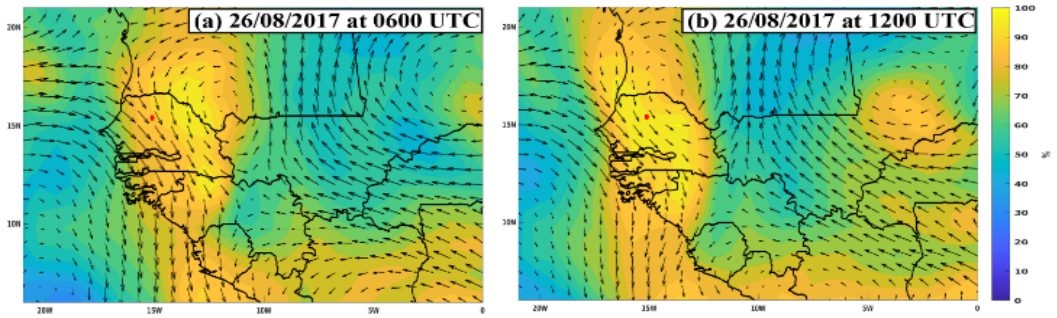

Figure 5. 700-hPa wind anomaly (vectors) and 700-hPa relative humidity (color) for 26/08/2017 at 0600UTC **(a)** and 1200UTC **(b)**. The red point represents the geographical position of Linguère.

Reference [34] showed, on a seasonal scale, that little precipitation occurs for PW values less than 30 mm. However, in areas of maximum precipitation, PW is greater than 50 mm. In Senegal, precipitation exists over a range from 35 to 60 mm of PW and there is a good correlation between PW and precipitation over Senegal [35]. In this study, the value of PW increased from 55 to 60 mm between 0600 UTC and 1200 UTC, in regions where the event took place, then reached the maximum value. Figure 4b, which represents the divergence of wind and relative humidity at 200-hPa, indicates a divergence around the area corresponding to cloud cover and a relative humidity reaching 100% around Linguère towards noon. This divergence in altitude induced by vertical transport and convergence in the lower layers (Figure 4(a)) indicates suitable conditions for the development of deep convection, thus giving a well-structured precipitating cloud system vertically.

Figure 5 shows the 31-day moving anomaly of the 700-hPa wind and relative humidity at the same pressure level. The presence of cyclonic circulation is also noticed at that level similar to the one at 850-hPa (Figure 3) with a north-westerly wind through to Linguère and maximum humidity in the western part of the vortex. At 0600UTC (Figure 5(a))the relative humidity had a value of around 90% near Linguère and then reached 100% at 1200 UTC (Figure 5(b)).

Figure 6 shows the Hovmoller diagram of 700-hPa relative vorticity obtained by averaging this parameteraround the latitudinal position of Linguère. As the system progressed from East to West this type of diagram allows to track the AEW progression during the event. A passage of a first AEW trough two days before (August 24, 2017) the event over Linguère is visible with a maximum vorticity value of $3.10^{-5}.s^{-1}$. A second AEW twice more intense than the previous one, with a vorticity reaching $6.10^{-5}.s^{-1}$, propagated toward Linguère on the day of the event with an average speed of 6.94 $m.s^{-1}$. In addition, a wave cut-off is observed and is consistent with the one shown by the extreme rain event occurred on September 1st, 2009, in Ouagadougou [14]. This configuration of AEW explains the recorded amount of humidity over the entire tropospheric column obtained around Linguère during the extreme rain event.

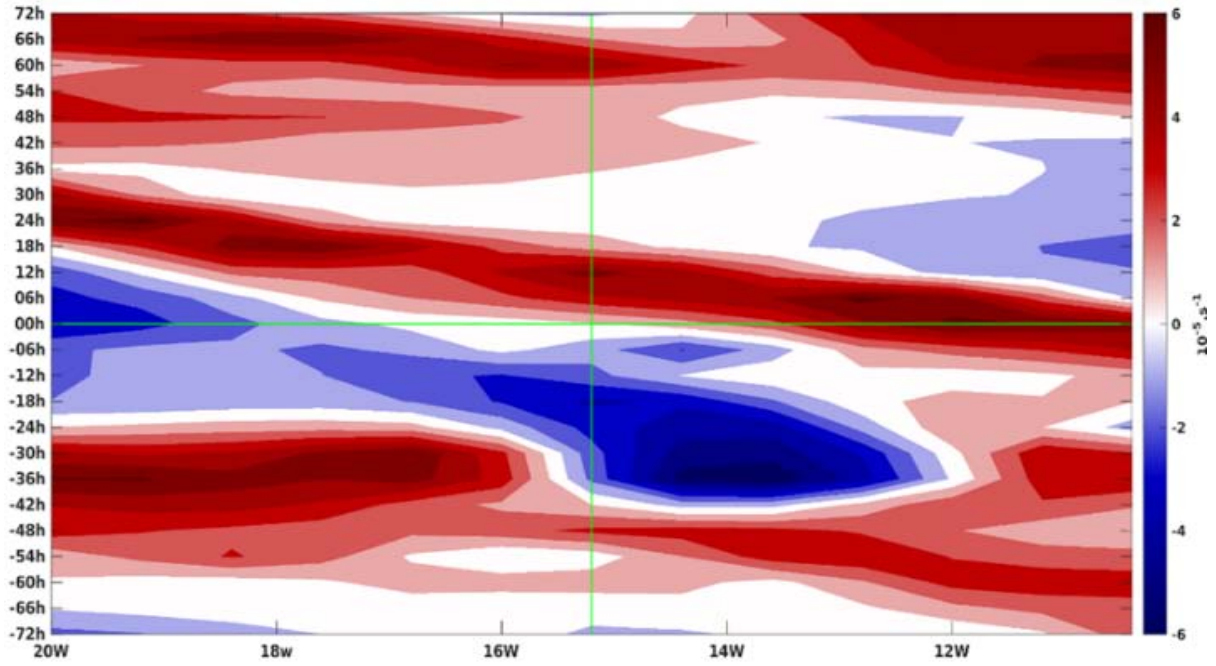

Figure 6. Hovmoller diagram of 700-hPa relative vorticity showing the evolution of two consecutive AEW troughs associated with the extreme rain in Linguère. The x-axis represents longitudes (degrees) and the y-axis shows the time related to the event (days). The vertical green line represents the longitude of Linguère and the horizontal green line represents the time when precipitation started.

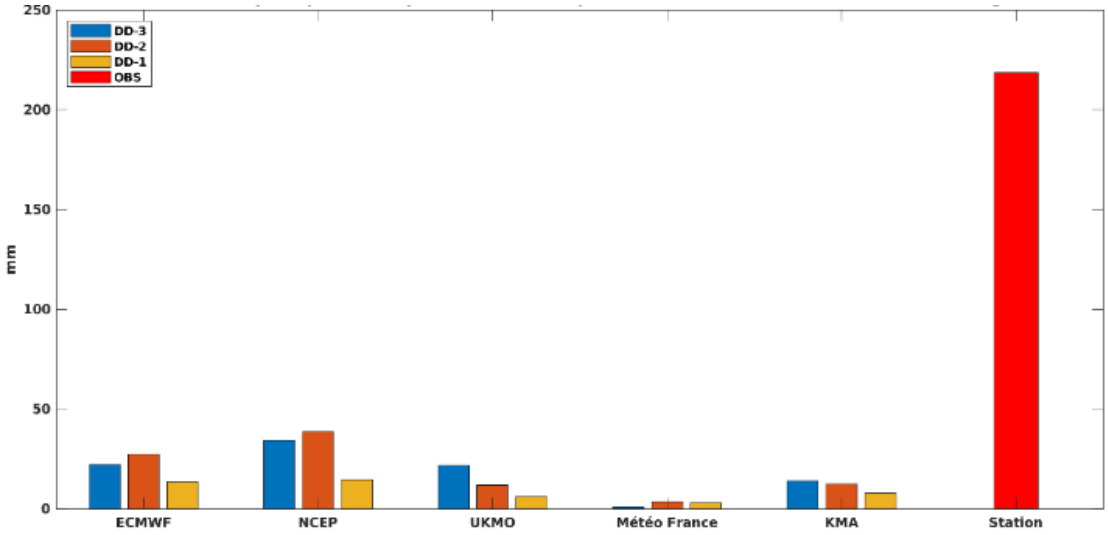

Figure 7. Forecast of daily accumulations of precipitation for August 26, 2017, in Linguère from operational forecast models.

4.3. Analysis of the Predictability of Numerical Forecast Models

A diagnosis of the predictability of five operational models for the three days preceding the events was carried out. Here for each model the calculation of the predicted daily cumulative precipitation for August 26, 2017, is done in the same way. The time interval considered for daily accumulation is between August 26 at 0000 UTC to August 27 at 0000 UTC and the forecast precipitations were averaged around the closest model grid points to Linguère's coordinates.

All models were initialized at 0000 UTC on August 24 (DD-3), August 25 (DD-2) and August 26 (DD-1). Figure 7 shows that each of the five models predicts weak precipitation amounts for the different initialization dates (DD-3, DD-2, and DD-1). We notice that the predicted amount of precipitation at DD-3 and DD-2 are generally higher than the one at DD-1. The NCEP model gives the most significant amounts of rain with less than 40 mm while Météo France simulates the lowest amounts with less than 5 mm.

In summary, the models used in this study are able to predict the short-term precipitation around Linguère; however, they tend to underestimate significantly the amount of rainfall compared to the ground station records (5 times less for the model with the largest quantity). The models could not bring out the character of a possible extreme rain event.

5. Conclusions

The objective of this work was to study the atmospheric

conditions associated with an extreme rain event listed in the database of the DPC of Senegal and caused significant socio-economic impacts. In this study the extreme events occurred at Linguère (Senegal) during August 26th, 2017 has been the focus. In-situ data provided by the ANACIM and TRMM rainfall data used to identify the event. For this, we first used the satellite observational dataset of BT and TRMM to analyze the spatio-temporal location of precipitation and convective systems. The data from the atmospheric reanalysis of ERA-Interim allowed us to see the behavior of certain atmospheric parameters during the extreme rain event. The performance of several numerical forecast models to predict the extreme event in the short term has been evaluated.

The results revealed that during normal days, recorded rainfall from ground station and satellite observation display comparable values; however, during the day of the extreme event, though the satellite identifie the event, it significantly underestimated its value. It is, therefore, important to improve the ground observations network in order to be able to document better the extremes events that have projected to continue to increase in the future [8,36]. We also note that the configuration of the simultaneous presence of low-level convergence humidity and 200-hPa wind divergence allows us to characterize the structure of occurrence of deep convection with a high precipitation rate during the day of the extreme rainfall. The structure of relative vorticity at 850 and 700-hPa provides a means to monitor the wave associated with the tropospheric instability. In addition, the presence of the wave caused excessive tropospheric humidity and provided synoptic forcing for the genesis of Meso-scale Convective Systems (MCS). The presence of high relative humidity at 700 and 200-hPa as well as Precipitable Water seems to be good indicators for extreme precipitation events.

With regard to the predictability of the event, the five numerical forecast models used were able to predict traces of precipitation in the short term (for the dates at DD-3, DD-2, and DD-1). However, the precipitation amount was underestimated compared to ground stations datasets.

It would be interesting to study several other cases for a better understanding and better prediction of such events.

References

[1] Barbé, L. (2002). Rainfall variability in West Africa during the years 1950-90. *J. Clim.***15** 16.

[2] Bell, M. A. and Lamb, P. J. (2006). Integration of Weather System Variability to Multidecadal Regional Climate Change: The West African Sudan-Sahel Zone, 1951-98. *J. Clim.***19** 5343-65.

[3] Lebel, T. and Ali, A. (2009). Recent trends in the Central and Western Sahel rainfall regime (1990-2007). *J. Hydrol.***375** 52-64.

[4] Descroix, L., Diongue Niang, A., Panthou, G., Bodian, A., Sane, Y., Dacosta, H., Malam Abdou, M., Vandervaere, J.-P. and Quantin, G. (2016). Évolution récente de la pluviométrie en Afrique de l'ouest à travers deux régions : la Sénégambie et le Bassin du Niger Moyen. *Climatologie*.

[5] Salack, S., Muller, B. and Gaye, A. T. (2011). Rain-based factors of high agricultural impacts over Senegal. Part I: integration of local to sub-regional trends and variability. *Theor. Appl. Climatol.***106** 1-22.

[6] Salack, S., Klein, C., Giannini, A., Sarr, B., Worou, O. N., Belko, N., Bliefernicht, J. and Kunstman, H. (2016). Global warming induced hybrid rainy seasons in the Sahel. *Environ. Res. Lett.***11** 104008.

[7] Ly, M., Traore, S. B., Alhassane, A. and Sarr, B. (2013). Evolution of some observed climate extremes in the West African Sahel. *Weather Clim. Extrem.***1** 19-25.

[8] Taylor, C. M., Belušić, D., Guichard, F., Parker, D. J., Vischel, T., Bock, O., Harris, P. P., Janicot, S., Klein, C. and Panthou, G. (2017). Frequency of extreme Sahelian storms tripled since 1982 in satellite observations. *Nature***544** 475-8.

[9] Sanogo, S., Fink, A. H., Omotosho, J. A., Ba, A., Redl, R. and Ermert, V. (2015). Spatio-temporal characteristics of the recent rainfall recovery in West Africa: RECENT RAINFALL RECOVERY IN WEST AFRICA. *Int. J. Climatol.***35** 4589-605.

[10] Douglas, I., Alam, K., Maghenda, M., Mcdonnell, Y., Mclean, L. and Campbell, J. (2008). Unjust waters: climate change, flooding and the urban poor in Africa. *Environ. Urban.***20** 187-205.

[11] Hartill, L. (2008). Understanding West Africa's rising food prices - Burkina Faso.ReliefWeb. Available at https://reliefweb.int/report/burkina-faso/understanding-west-africas-rising-food-prices.

[12] Cornforth, R., Mumba, Z., Parker, D. J., Berry, G., Chapelon, N., Diakaria, K., Diop-Kane, M., Ermert, V., Fink, A. H., Knippertz, P., Lafore, J. P., Laing, A., Lepape, S., Maidment, R., Methven, J., Orji, B., Osika, D., Poan, E., Roca, R., Rowell, S., Smith, R., Spengler, T., Taylor, C. M., Thorncroft, C., Vincendon, J.-C., Yorke, C. and Thorncroft, C. (2017). Synoptic Systems. In *Meteorology of Tropical West Africa* (D. J. Parker and M. Diop-Kane, ed) pp 40-89. John Wiley & Sons, Ltd, Chichester, UK.

[13] Lafore, J.-P., Beucher, F., Peyrillé, P., Diongue - Niang, A., Chapelon, N., Bouniol, D., Caniaux, G., Favot, F., Ferry, F., Guichard, F., Poan, E., Roehrig, R. and Vischel, T. (2017). A multi-scale analysis of the extreme rain event of Ouagadougou in 2009. *Q. J. R. Meteorol. Soc.***143** 3094-109.

[14] Engel, T., Fink, A., Knippertz, P., Pante (né Gläser), G. and Bliefernicht, J. (2017). Extreme Precipitation in the West African Cities of Dakar and Ouagadougou: Atmospheric Dynamics and Implications for Flood Risk Assessments. *J. Hydrometeorol.***18** 2937-57.

[15] Janicot, S., Caniaux, G., Chauvin, F., deCoëtlogon, G., Fontaine, B., Hall, N., Kiladis, G., Lafore, J. P., Lavaysse, C., Lavender, S. L., Leroux, S., Marteau, R., Mounier, F., Philippon, N., Roehrig, R., Sultan, B. and Taylor, C. M. (2011). Intraseasonal variability of the West African monsoon. *Atmospheric Sci. Lett.***12** 58-66.

[16] Lafore, J.-P., Flamant, C., Guichard, F., Parker, D. J., Bouniol, D., Fink, A. H., Giraud, V., Gosset, M., Hall, N., Höller, H., Jones, S. C., Protat, A., Roca, R., Roux, F., Saïd, F. and Thorncroft, C. (2011). Progress in understanding of weather systems in West Africa. *Atmospheric Sci. Lett.***12** 7-12.

[17] Nicholson, S. E. (2013). The West African Sahel: A Review of Recent Studies on the Rainfall Regime and Its Interannual Variability. *ISRN Meteorol.***2013** 1-32.

[18] Sane, Y., Panthou, G., Bodian, A., Vischel, T., Lebel, T., Dacosta, H., Quantin, G., Wilcox, C., Ndiaye, O., Diongue-Niang, A. and Diop Kane, M. (2018). Intensity-duration-frequency (IDF) rainfall curves in Senegal. *Nat. Hazards Earth Syst. Sci.***18** 1849-66.

[19] Diop, L., Bodian, A. and Diallo, D. (2016). Spatiotemporal Trend Analysis of the Mean Annual Rainfall in Senegal. *Eur. Sci. J. ESJ* **12** 231.

[20] Huffman, G. J., Bolvin, D. T., Nelkin, E. J., Wolff, D. B., Adler, R. F., Gu, G., Hong, Y., Bowman, K. P. and Stocker, E. F. (2007). The TRMM Multisatellite Precipitation Analysis (TMPA): Quasi-Global, Multiyear, Combined-Sensor Precipitation Estimates at Fine Scales. *J. Hydrometeorol.* **8** 38-55.

[21] Nicholson, S. E., Some, B., Mccollum, J., Nelkin, E., Klotter, D., Berte, Y., Diallo, B. M., Gaye, I., Kpabeba, G., Ndiaye, O., Noukpozounkou, J. N., Tanu, M. M., Thiam, A., Toure, A. A. and Traore, A. K. (2003). Validation of TRMM and Other Rainfall Estimates with a High-Density Gauge Dataset for West Africa. Part I: Validation of GPCC Rainfall Product and Pre-TRMM Satellite and Blended Products. *J. Appl. Meteorol.* **42** 18.

[22] Maggioni, V., Meyers, P. C. and Robinson, M. D. (2016). A Review of Merged High-Resolution Satellite Precipitation Product Accuracy during the Tropical Rainfall Measuring Mission (TRMM) Era. *J. Hydrometeorol.***17** 1101-17.

[23] ZULKAFLI, Z., BUYTAERT, W., ONOF, C., MANZ, B., TARNAVSKY, E., LAVADO, W. and GUYOT, J.-L. (2014). A Comparative Performance Analysis of TRMM 3B42 (TMPA) Versions 6 and 7 for Hydrological Applications over Andean-Amazon River Basins. *J. Hydrometeorol.***15** 581-92.

[24] PRAKASH, S., MITRA, A. K., MOMIN, I. M., PAI, D. S., RAJAGOPAL, E. N. and BASU, S. (2015). Comparison of TMPA-3B42 Versions 6 and 7 Precipitation Products with Gauge-Based Data over India for the Southwest Monsoon Period. *J. Hydrometeorol.* **16** 346-62.

[25] JOYCE, R., JANOWIAK, J. and HUFFMAN, G. (2001). Latitudinally and Seasonally Dependent Zenith-Angle Corrections for Geostationary Satellite IR Brightness Temperatures. *J. Appl. Meteorol.***40** 689-703.

[26] FUNK, C., PETERSON, P., LANDSFELD, M., PEDREROS, D., VERDIN, J., SHUKLA, S., HUSAK, G., ROWLAND, J., HARRISON, L., HOELL, A. and MICHAELSEN, J. (2015). The climate hazards infrared precipitation with stations - A new environmental record for monitoring extremes. *Sci. Data***2** 150066.

[27] DEE, D. P., UPPALA, S. M., SIMMONS, A. J., BERRISFORD, P., POLI, P., KOBAYASHI, S., ANDRAE, U., BALMASEDA, M. A., BALSAMO, G., BAUER, P., BECHTOLD, P., BELJAARS, A. C. M., VAN DEBERG, L., BIDLOT, J., BORMANN, N., DELSOL, C., DRAGANI, R., FUENTES, M., GEER, A. J., HAIMBERGER, L., HEALY, S. B., HERSBACH, H., HÓLM, E. V., ISAKSEN, L., KÅLLBERG, P., KÖHLER, M., MATRICARDI, M., MCNALLY, A. P., MONGE-SANZ, B. M., MORCRETTE, J.-J., PARK, B.-K., PEUBEY, C., DEROSNAY, P., TAVOLATO, C., THÉPAUT, J.-N. and VITART, F. (2011). The ERA-Interim reanalysis: configuration and performance of the data assimilation system. *Q. J. R. Meteorol. Soc.***137** 553-97.

[28] ROCA, R., CHAMBON, P., JOBARD, I., KIRSTETTER, P.-E., GOSSET, M. and BERGÈS, J. C. (2010). Comparing Satellite and Surface Rainfall Products over West Africa at Meteorologically Relevant Scales during the AMMA Campaign Using Error Estimates. *J. Appl. Meteorol. Climatol.***49** 715-31.

[29] MATHON, V. and LAURENT, H. (2001). Life cycle of Sahelian mesoscale convective cloud systems. *Q. J. R. Meteorol. Soc.***127** 377-406.

[30] REED, R. J., NORQUIST, D. C. and RECKER, E. E. (1977). The Structure and Properties of African Wave Disturbances as Observed During Phase III of GATE. *Mon. Weather Rev.***105** 317-33.

[31] PAYNE, S. W. and MCGARRY, M. M. (1977). The relationship of satellite inferred convective activity to easterly waves over west africa and the adjacent ocean during phase iii of gate. *Mon Wea Rev* 105: 413.

[32] DIEDHIOU, A., JANICOT, S., VILTARD, A., DEFELICE, P. and LAURENT, H. (1999). Easterly wave regimes and associated convection over West Africa and tropical Atlantic: results from the NCEP/NCAR and ECMWF reanalyses. *Clim. Dyn.***15** 795-822.

[33] KILADIS, G. N., THORNCROFT, C. D. and HALL, N. M. J. (2006). Three-Dimensional Structure and Dynamics of African Easterly Waves. Part I: Observations. *J. Atmospheric Sci.***63** 2212-30.

[34] BOCK, O., BOUIN, M. N., DOERFLINGER, E., COLLARD, P., MASSON, F., MEYNADIER, R., NAHMANI, S., KOITÉ, M., GAPTIA LAWAN BALAWAN, K., DIDÉ, F., OUEDRAOGO, D., POKPERLAAR, S., NGAMINI, J.-B., LAFORE, J. P., JANICOT, S., GUICHARD, F. and NURET, M. (2008). West African Monsoon observed with ground-based GPS receivers during African Monsoon Multidisciplinary Analysis (AMMA). *J. Geophys. Res.***113** D21105.

[35] POAN, D. E. (2013). Documentation et interprétation physique de la variabilité intrasaisonnière de la mousson africaine; application à la prévision.Available at http://ethesis.inp-toulouse.fr/archive/00002653/.

[36] SYLLA, M. B., ELGUINDI, N., GIORGI, F. and WISSER, D. (2016). Projected robust shift of climate zones over West Africa in response to anthropogenic climate change for the late 21st century. *Clim. Change***134** 241-53.